Mitoxantrone, pixantrone, and mitoxantrone (2-hydroxyethyl)piperazine are toll-like receptor 4 antagonists, þÿinhibit NF-ºB activation, and decrease TNF-alph primary microglia

Rinne, Maiju Kaarina

2020-11-01

Rinne , M K , Mätlik , K , Ahonen , T J , Vedovi , F , Zappia , G , Moreira , V M , Yli-Kauhaluoma , J T , Leino , S , Salminen , O S , Kalso , E A , Airavaara , M T & Xhaard , H G M 2020 , ' Mitoxantrone, pixantrone, and mitoxantrone (2-hydroxyethyl)piperazine are þÿtoll-like receptor 4 antagonists, inhibit NF-ºB activation, and decrease in primary microglia ' , European Journal of Pharmaceutical Sciences , vol. 154 , no. 1.11.2020 , 105493 . https://doi.org/10.1016/j.ejps.2020.105493

http://hdl.handle.net/10138/333041
https://doi.org/10.1016/j.ejps.2020.105493

Mitoxantrone, pixantrone and mitoxantrone (2-hydroxyethyl)piperazine are toll-like receptor 4 antagonists, inhibit NF-κB activation, and decrease TNF-alpha secretion in primary microglia

Maiju Rinne Conceptualization; Data curation; Formal analysis; Investigation; Methodology; Supervision; Validation
Kert Mätlik Conceptualization; Data curation; Formal analysis; Investigation; Methodology; Supervision; Writing - re
Tiina Ahonen Formal analysis; Validation; Writing - review & editing ,
Fabio Vedovi Conceptualization; Data curation; Formal analysis; Visualization; Roles/Writing - original draft; Writing
Giovanni Zappia Conceptualization; Funding acquisition; Supervision; Writing - review & editing ,
Vânia M. Moreira Conceptualization; Funding acquisition; Supervision; Writing - review & editing ,
Jari Yli-Kauhaluoma Conceptualization; Funding acquisition; Project administration; Supervision; Writing - review &
Sakari Leino Formal analysis; Investigation; Visualization; Writing - review & editing ,
Outi Salminen Formal analysis; Investigation; Visualization; Writing - review & editing ,
Eija Kalso Conceptualization; Funding acquisition; Project administration; Supervision; Writing - review & editing ,
Mikko Airavaara Conceptualization; Funding acquisition; Investigation; Methodology; Project administration; Resou
Henri Xhaard Conceptualization; Funding acquisition; Investigation; Methodology; Project administration; Resource

PII: S0928-0987(20)30282-7
DOI: https://doi.org/10.1016/j.ejps.2020.105493
Reference: PHASCI 105493

To appear in: *European Journal of Pharmaceutical Sciences*

Received date: 22 January 2020
Revised date: 22 July 2020
Accepted date: 27 July 2020

Please cite this article as: Maiju Rinne Conceptualization; Data curation; Formal analysis; Investigation; Methodolog
Kert Mätlik Conceptualization; Data curation; Formal analysis; Investigation; Methodology; Supervision; Writing - re
Tiina Ahonen Formal analysis; Validation; Writing - review & editing , Fabio Vedovi Conceptualization; Data curatio
Giovanni Zappia Conceptualization; Funding acquisition; Supervision; Writing - review & editing ,
Vânia M. Moreira Conceptualization; Funding acquisition; Supervision; Writing - review & editing ,
Jari Yli-Kauhaluoma Conceptualization; Funding acquisition; Project administration; Supervision; Writing - review &
Sakari Leino Formal analysis; Investigation; Visualization; Writing - review & editing ,
Outi Salminen Formal analysis; Investigation; Visualization; Writing - review & editing ,
Eija Kalso Conceptualization; Funding acquisition; Project administration; Supervision; Writing - review & editing ,
Mikko Airavaara Conceptualization; Funding acquisition; Investigation; Methodology; Project administration; Resou
Henri Xhaard Conceptualization; Funding acquisition; Investigation; Methodology; Project administration; Resource
Mitoxantrone, pixantrone and mitoxantrone (2-hydroxyethyl)piperazine are toll-like receptor 4 antagonists, inhibit NF-κB activation, and decrease TNF-alpha secretion in primary microglia, *European Journal of Pharmaceutical Sciences* (2020), doi: https://doi.org/10.1016/j.ejps.2020.105493

Mitoxantrone, pixantrone and mitoxantrone (2-hydroxyethyl)piperazine are toll-like receptor 4 antagonists, inhibit NF-κB activation, and decrease TNF-alpha secretion in primary microglia

Maiju Rinne[a], Kert Mätlik[b,c], Tiina Ahonen[a], Fabio Vedovi [a,d], Giovanni Zappia[d], Vânia M. Moreira[a,e,f,g], Jari Yli-Kauhaluoma[a], Sakari Leino[h], Outi Salminen[h], Eija Kalso[c,i], Mikko Airavaara[b*], Henri Xhaard[a*]

[a]Drug Research Program, Division of Pharmaceutical Chemistry and Technology, Faculty of Pharmacy, University of Helsinki, FI-00014 Helsinki, Finland

[b]Institute of Biotechnology, HiLIFE, University of Helsinki, FI-00014 Helsinki, Finland

[c]Department of Pharmacology, Faculty of Medicine, University of Helsinki, FI-00014 Helsinki, Finland

[d]Department of Biomolecular Sciences, University Urbino Carlo Bo, P.zza Rinascimento, 6 61029 Urbino (PU), Italy

[e]Strathclyde Institute of Pharmacy and Biomedical Sciences, University of Strathclyde, G4 0RE Glasgow, U.K.

[f]Laboratory of Pharmaceutical Chemistry, Faculty of Pharmacy, University of Coimbra, 3004-548 Coimbra, Portugal

[g]Center for Neuroscience and Cell Biology, University of Coimbra, 3004-504 Coimbra, Portugal

[h]Drug Research Program, Division of Pharmacology and Pharmacotherapy, Faculty of Pharmacy, University of Helsinki, FI-00014 Helsinki, Finland

[i]Department of Anaesthesiology, Intensive Care and Pain Medicine, University of Helsinki and Helsinki University Hospital. FI-00029 HUS, Finland

*** Correspondence** (Airavaara and Xhaard contributed equally to this work):
Henri Xhaard
henri.xhaard@helsinki.fi

Declarations of interest: none

Abstract

Toll-like receptor 4 (TLR4) recognizes various endogenous and microbial ligands and is an essential part in the innate immune system. TLR4 signaling initiates transcription factor NF-κB and production of proinflammatory cytokines. TLR4 contributes to the development or progression of various diseases including stroke, neuropathic pain, multiple sclerosis, rheumatoid arthritis and cancer, and better therapeutics are currently sought for these conditions. In this study, a library of 140 000 compounds was virtually screened and a resulting hit-list of 1000 compounds was tested using a cellular reporter system. The topoisomerase II inhibitor mitoxantrone and its analogues pixantrone and mitoxantrone (2-hydroxyethyl)piperazine were identified as inhibitors of TLR4 and NF-κB activation. Mitoxantrone was shown to bind directly to the TLR4, and pixantrone and mitoxantrone (2-hydroxyethyl)piperazine were shown to inhibit the production of proinflammatory cytokines such as tumor necrosis factor alpha (TNFα) in primary microglia. The inhibitory effect on NF-κB activation or on TNFα production was not mediated through cytotoxity at ≤ 1 μM concentration, as assessed by ATP counts for mitoxantrone, pixantrone and mitoxantrone (2-hydroxyethyl)piperazine treated cells. This study thus identifies a new mechanism of action for mitoxantrone, pixantrone, and mitoxantrone (2-hydroxyethyl)piperazine through the TLR4.

Keywords:

Mitoxantrone, pixantrone, mitoxantrone (2-hydroxyethyl)piperazine, toll-like receptor 4, virtual screening, NF-κB

Abbreviations:

TLRs: toll-like receptors; TLR4: toll-like receptor 4; NF-κB: nuclear factor kappa B; TNFα: tumor necrosis factor alpha; PAMPs: pathogen-associated molecular patterns; LPS: lipopolysaccharide; DAMPs: damage-associated molecular patterns; HMGB1: high mobility group box 1; MS: multiple sclerosis; TIR-domain: toll/interleukin-1 receptor homology domain; MD-2: myeloid differentiation factor 2; SEAP: secreted embryonic alkaline phosphatase; PMA: phorbol 12-myristate 13-acetate; DMSO: dimethyl sulfoxide; DMEM: Dulbecco's Modified Eagle's Medium; HBSS: Hanks's balanced salt solution; PKC: protein kinase C

1 Introduction

Toll-like receptors (TLRs) belong to the family of pattern recognition receptors (Jeannin et al., 2008) and are mediators of innate immune system activation. Thirteen mammalian TLRs have been identified, and ten of them are functional in human. TLRs recognize various ligands (Janssens and Beyaert, 2003; Kanzler et al., 2007). These ligands are for a large part of microbial origin, referred to as pathogen-associated molecular patterns (PAMPs), of which, lipopolysaccharide (LPS) from Gram-negative bacteria is a prominent example. In addition, TLRs recognize various endogenous ligands called damage-associated molecular patterns (DAMPs) that include such as heat-shock proteins, β-defensins and high mobility group box 1 (HMGB1).

TLR4 has received considerable attention in recent years, mostly because of its therapeutic potential. TLR4 is widely expressed in periphery, but also in CNS, mostly in astrocytes and microglia (Vaure and Liu, 2014), and it is involved in the development/maintenance of chronic pain and neuroinflammation (Kuang et al., 2012; Nicotra et al., 2012; Tanga et al., 2005), multiple sclerosis (MS) (Miranda-Hernandez and Baxter, 2013), rheumatoid arthritis (Maciejewska Rodrigues et al., 2009), cancer (Oblak and Jerala, 2011), and tissue damages after stroke (Hyakkoku et al., 2010; Tang et al., 2007). All these conditions are in high need for better therapeutic compounds. As an example, chronic pain is affecting up to 1.5 billion of people and is responsible for one of the highest expenses in health care systems worldwide (Jacobs, 2005). It results from complex pathological processes, of which neuronal and non-neuronal cells - such as microglia and astrocytes - are involved. A significant role of the inflammatory system has been identified in the development and maintenance of chronic pain including neuropathic pain (Grace et al., 2011; Meller et al., 1994; Milligan and Watkins, 2009; Watkins et al., 1997) and opioid-induced hyperalgesia and tolerance (Mattioli et al., 2014). More specifically, TLR4-mediated microglial activation has been shown to be one of the initiators in the development of neuropathic and chronic pain (Kuang et al., 2012; Nicotra et al., 2012; Tanga et al., 2005). Conversely, reduced production of proinflammatory cytokines, seen in animal models lacking TLR4 or achieved via blocking TLR4 with small molecules, has a reducing effect on inflammatory and neuropathic pain (Liu et al., 2012; Sommer et al., 1999; Sorge et al., 2011; Wu et al., 2010, 2015; Zhou et al., 2018). Another example, MS, is an autoimmune disease and one of the most common neurologic disorder. Toll-like receptors in the innate immune system are involved in the development of autoimmune inflammation (O'Brien et al., 2008). TLR4s and endogenous ligand HMGB1 are highly expressed in MS patients (Andersson et al., 2008), but association between the receptor and disease has remained unclear (Kroner et al., 2005; Reindl et al., 2003).

TLRs act as units by forming homo- or heteromers, and crystal structures have been characterized for most of the TLRs. TLRs share the same protein fold through species from invertebrates to vertebrates (Rock et al., 1998). Leucine-rich repeats form a horseshoe-like extracellular domain, which participates in ligand binding and recognition (Akira et al., 2006). The extracellular domain is joined together with an intracellular toll/interleukin-1 receptor homology domain (TIR-domain) (Kawai and Akira, 2009), which activates signaling pathways. The extracellular domain and TIR-domain are connected by a single alpha-helical transmembrane domain.

Upon activation TLR4 forms a complex with the co-ligand and helper protein myeloid differentiation factor 2 (MD-2, also referred to as lymphocyte antigen 96). The dimerization of this TLR4 unit causes activation of the signaling pathway by bringing together intracellular TIR-domains. This complex further recruits cytoplasmic adaptor proteins, such as myeloid differentiation primary response 88 (MyD88), TIR domain-containing adaptor protein (TIRAP) and TIR-domain-containing adapter-inducing interferon-β (TRIF), leading to activation of various protein kinases and transcription factors (Akira et al., 2003). Downstream of the TLR4 signaling

cascade (Lu et al., 2008), the transcription factor NF-κB is one of the most important modulators of the activation of the innate immune system. NF-κB is in charge of the production of various secreted proteins called proinflammatory cytokines, including TNFα and interleukin 1β (IL-1β) that are essential for an effective immune response (Baeuerle and Henkel, 1994; Peri and Piazza, 2012).

A three-dimensional structure of a complex of human TLR4, MD-2 and LPS has been solved by X-ray crystallography (PDB code: 3FXI) (Park et al., 2009). The helper protein MD-2 consists of β-sheets that are surrounding a hydrophobic pocket for ligand binding. LPS binds to this pocket with its lipid chains, and causes the formation of the TLR4 and MD-2 complex. MD-2 undergoes conformational changes upon dimerization with TLR4, having one of its loops, the F126 loop, forming polar interactions with TLR4. LPS forms a direct bridge between TLR4 and MD-2. LPS has six lipid chains, of which five bind into the hydrophobic pocket of MD-2 and one forms a hydrophobic interaction with conserved phenylalanines (Phe-440, Phe-463) of TLR4.

Only few high-affinity small molecule ligands of TLR4 had been reported when we started the study in 2013. The TLR4-specific small molecule antagonist ethyl (6*R*)-6-[(2-chloro-4-fluorophenyl)sulfamoyl]cyclohexene-1-carboxylate (TAK-242) (**Figure 1**) advanced to clinical trials for the treatment of sepsis, but it failed to show therapeutic effect (Rice et al., 2010). TAK-242 has been suggested to bind covalently to the intracellular domain of TLR4, more specifically to Cys-747 (Matsunaga et al., 2011; Takashima et al., 2009), and to trap the receptor in an inactive state by interfering with protein-protein interactions of adaptor proteins. In addition, β-amino alcohol derivatives (**Figure 1**) (Bevan et al., 2010; Chavez et al., 2011) have been reported to target and inhibit TLR4 by binding to MD-2 loop site and disrupting the formation of the TLR4 and MD-2 complex. β-amino alcohol derivatives alone did not have analgesic effect, but they potentiated the analgesic effect of morphine by inhibiting morphine-induced TLR4 activation (Bevan et al., 2010). Some lipid mimetics have been found to have an inhibitory effect on TLR4 (Meng et al., 2010). These compounds aimed at mimicking the glycolipid part of LPS to maintain the selectivity and potency towards TLR4. However, mimetics often come with the disadvantage of large size that limits their use as drugs. Lipid mimetics are commonly known to bind to the LPS-binding site in TLR4 and/or MD-2 (Ohto et al., 2012; Scior et al., 2013). The TLR4 specific lipid mimetic antagonist, [(2*R*,3*R*,4*R*,5*S*,6*R*)-4-decoxy-5-hydroxy-6-[[(2*R*,3*R*,4*R*,5*S*,6*R*)-4-[(3*R*)-3-methoxydecoxy]-6-(methoxymethyl)-3-[[(*Z*)-octadec-11-enoyl]amino]-5-phosphonooxyoxan-2-yl]oxymethyl]-3-(3-oxotetradecanoylamino)oxan-2-yl] dihydrogen phosphate (eritoran) (Mullarkey et al., 2002), reached clinical trials in severe sepsis, but did not show therapeutic effect (Opal et al., 2013).

In this study, a virtual screen on a library of 140 000 compounds was conducted, a hit list of 1000 compounds was tested by experimental screening using a cellular reporter assay, and the hits from the experimental screening were further validated. After validation of the hits from primary experimental screen, one positive hit was found, mitoxantrone (1,4-dihydroxy-5,8-bis[2-(2-hydroxyethylamino)ethylamino]anthracene-9,10-dione) (**Figure 1**), which was further investigated more in details together with two commercially available derivatives, mitoxantrone (2-hydroxyethyl)piperazine (8,11-dihydroxy-4-(2-hydroxyethyl)-6-[2-(2-hydroxyethylamino)ethylamino]-2,3-dihydro-1*H*-naphtho[3,2-*f*]quinoxaline-7,12-dione) (**Figure 1**). The biological effect of the compounds through TNFα production was assessed in primary microglia from mouse. Furthermore, a direct binding mechanism to the target receptor was demonstrated using [^{3}H]mitoxantrone on TLR4 expressing membrane fractions from the HEK-Blue™-hTLR4 cell line.

2 Materials and Methods

Virtual screening – The crystal structure of TLR4 with the co-crystallized ligand LPS was used (PDB code: 3FXI (Park et al., 2009)). As the starting point to identify novel antagonists for TLR4, a library of ca. 140 000 compounds (https://www.fimm.fi/en/services/technology-centre/htb/equipment-and-libraries/chemical-libraries, October 2015) was screened virtually. The library includes for example a subset of approved drug molecules (ca. 640 compounds), natural products (ca. 1 000), and a set of diverse drug-like compounds (ca. 50 000). The library was converted into 3D format using Maestro (LigPrep) and Canvas by Schrödinger ("Schrödinger Release 2015-3: Maestro, Version 10.3, Schrödinger, LLC, New York, NY.," 2015) at pH 7.4 with standard parameters. The library preparation allows creation of ionic and tautomeric forms. For compounds of undefined chirality, a single enantiomer was randomly kept in order to avoid creating a representation bias and in the same time to limit the size of the prepared library for docking. Upon analysis of the hit lists, duplicates were automatically removed, as well as compounds with substructures prone to chemical reactivity and pan-assay interference (Baell and Nissink, 2018; Rishton, 1997).

All virtual screens were hampered by the scarcity of active compounds to be used as references. Therefore, a relatively large (1000 compounds) hit-list was built to be experimentally tested. Five independent screens were conducted, each leading to a hit list of 200 compounds: one by similarity search, two by pharmacophore, and two by docking. All of the methods produced ranked lists, which were filled up to 200 compounds, if the initial compounds were removed e.g. because of the presence in duplicate lists or physical unavailability.

For the ligand-based similarity search, a known racemic β-amino alcohol-derived TLR4 antagonist, 1-[[[1-(2-chlorobenzyl)-3,5-dimethyl-1*H*-pyrazol-4-yl]methyl](methyl)amino]-3-(4-chlorophenoxy)propan-2-ol, was used (Bevan et al., 2010) as a starting point (**Figure 1**). The search was based on molecular Fingerprints (Willett, 2003) ranked using a Tanimoto similarity coefficient of Discovery Studio v4.5 (BIOvIA, 2015: Dassault Systèmes, San Diego, CA, USA). Pharmacophore modeling was also conducted using DiscoveryStudio v4.5. For the pharmacophore-based and docking-based screens, small-molecule antagonists were hypothesized either compete for the LPS binding site or for the MD-2 loop binding site in TLR4; leading to four independent hit lists. Pharmacophoric features were selected manually using Maestro 10.3 [Schrödinger] and PyMol 1.7.0.0 (PyMOL 1.7.0.0 Schrödinger, n.d.) (shown in **Figure 2**). Features were selected based on key interactions to TLR4 obtained from X-ray structure (Park et al., 2009), five features for LPS and eight features for MD-2 loop were determined. Independent screens were performed for both pharmacophores, and compounds were selected to match at least four of the features.

Docking-based virtual screening was conducted using Glide SP [Schrödinger] with standard parameters. The grid generation for the docking-based screens was based on an area of 10 Å around key amino acids in LPS binding site or in MD-2 loop site in TLR4 (shown in **Figure 3**). The complete library (140 000 compounds) was docked to both the LPS and MD-2 binding sites, to mimic the binding of the co-ligand or the helper protein. Compounds were ranked based on their docking scores (GlideXP).

2.1 Experimental screening using a gene-reporter assay

The primary experimental screen was conducted for the 1 000 compounds that could be physically obtained following the five virtual screens. Compounds were obtained through acoustic dispensing and tested in 384-well plate format. The HEK-Blue™-hTLR4 (cat. no. hkb-htlr4, InvivoGen) cell line, co-expressing the human MD-2 and CD14, was used and the level of TLR4 activation was determined by measuring the level of secreted embryonic alkaline phosphatase (SEAP) activity in

the cell culture medium. In the HEK-Blue™-hTLR4 cell line, the SEAP reporter gene is downstream of NF-κB and AP1 binding sites. Cells were cultivated at 37°C in 5% CO_2 in an air-ventilated humidified incubator, in Dulbecco's Modified Eagle's Medium (DMEM) supplemented with 10% fetal bovine serum (FBS), 0.2% Normocin™ and 0.4% HEKBlue selection antibiotics. For testing, the cells were plated in DMEM supplemented with 0.5% FBS and antibiotics using a BRAD (BioTek MultiFlo FX with Random Access Dispensing technology) dispenser. After an overnight incubation, the compounds were added from matrix plates (BioMek FXp), two replica wells for each compound, at 5 µM concentration, and incubated for 30 min before LPS was added (sonic dispension with ECHO). TAK-242 was used as a positive control, to show full inhibition of TLR4 activation. 1 ng/mL LPS-EK Ultrapure (cat. code tlrl-peklps, InvivoGen) was used for submaximal activation of TLR4 (signal/background *S/B*=5.0, *Z'*=0.66; 10 ng/mL LPS producing *S/B*=8.8). On the next day NovaBright™ (cat. no. N10578, NovaBright Phospha-Light EXP Assay Kit for SEAP, Invitrogen) reagent buffer was added to assay plates (nonplacental alkaline phosphatase activity inhibition) (BRAD) and followed by medium addition (BioMek FXp). Assay plates were sealed, incubated for 5 min, at 65 °C, and equilibrated to room temperature. NovaBright™ assay reagent was added (BRAD) and plates incubated for 20 min at room temperature. The SEAP signal was measured as a TLR4 activation signal for 0.1-1 s/well (luminescence, Pherastar FS). To measure cytotoxicity, ATP was measured from the cells using the CellTiter-Glo® (cat. no. G7570, Promega) reagent according to manufacturer's protocol (luminescence, Pherastar FS).

2.2 Validation of positive hits

Compounds were repurchased from independent suppliers (Biovision: vatalanib (*N*-(4-chlorophenyl)-4-(pyridin-4-ylmethyl)phthalazin-1-amine), mitoxantrone, pixantrone; Abcam: banoxantrone (2-[[4-[2-[dimethyl(oxido)azaniumyl]ethylamino]-5,8-dihydroxy-9,10-dioxoanthracen-1-yl]amino]-*N*,*N*-dimethylethanamine oxide), benazepril (2-[(3*S*)-3-[[(2*S*)-1-ethoxy-1-oxo-4-phenylbutan-2-yl]amino]-2-oxo-2,3,4,5-tetrahydro-1*H*-1-benzazepin-1-yl]acetic acid), salicin ((2*R*,3*S*,4*S*,5*R*,6*S*)-2-(hydroxymethyl)-6-[2-(hydroxymethyl)phenoxy]oxane-3,4,5-triol); Carbosynth: mitoxantrone (2-hydroxyethyl)piperazine; ChemBridge: CAS610281-22-6 (1-(4-chloro-2-methylphenoxy)-3-[(1-phenylethyl)amino]-2-propanol); Specs: CAS900453-15-8 (7-benzyl-2-[[(4-chlorophenyl)amino]methyl]-5,6,7,8-tetrahydropyrido[4',3':4,5]thieno[2,3-*d*]pyrimidin-4(3*H*)-one); Akos: CAS1021989-35-4 (*N*-(9-ethyl-9*H*-carbazol-3-yl)-N^2-methylglycinamide), SigmaAldrich: (-)-etoposide ((5*S*,5a*R*,8a*R*,9*R*)-5-[[(2*R*,4a*R*,6*R*,7*R*,8*R*,8a*S*)-7,8-dihydroxy-2-methyl-4,4*a*,6,7,8,8*a*-hexahydropyrano[3,2-*d*][1,3]dioxin-6-yl]oxy]-9-(4-hydroxy-3,5-dimethoxyphenyl)-5a,6,8*a*,9-tetrahydro-5*H*-[2]benzofuro[6,5-*f*][1,3]benzodioxol-8-one), InvivoGen: TAK-242) (**Figure 4** and **1)**. The identity of compounds was independently verified with ultra-performance liquid chromatography – high resolution mass spectrometry (Waters Acquity® UPLC system attached to Acquity PDA detector and Waters Synapt G2 HDMS mass spectrometer) or nuclear magnetic resonance (NMR) spectroscopy (Bruker Ascend 400 spectrometer). Validation of the hits from the first experimental screen was done with a dose-response analysis. HEK-Blue™-hTLR4 cells were cultivated and plated as previously. 9000 cells/well were plated on clear 96-well plates (cat. no. 655180, CELLSTAR®, Greiner Bio-One), leaving the outer wells cell-free and filled with sterile water to minimize evaporation. After overnight incubation, the compounds were added in DMEM supplemented with 0.5% FBS with final concentrations of 5 µM, 1 µM and 500 nM, and incubated for 30 min prior to stimulation with LPS or phorbol 12-myristate 13-acetate (PMA, a TLR4-independent NF-κB activator, cat. no. tlrl-pma, InvivoGen). After 22 hours of incubation, the media was collected and added to a 96-well opaque plate (cat. no. 6005290, Optiplate-96, PerkinElmer). Novabright™ assay buffer was added and incubated for 5 min, at 65 °C and equilibrated to room temperature as previously. Novabright™ reagent buffer was added and incubated for 20 min at room temperature in a dark condition, and the

SEAP-signal was detected (FLUOstar OPTIMA, BMG Labtech). Cell viability was controlled with the CellTiter-Glo® luminescent cell viability assay as reported above (FLUOstar OPTIMA, BMG Labtech).

2.3 TNFα detection

To further investigate the biological effect of the compounds, an ELISA-based (cat. no. 88-7324-22, Invitrogen) detection of TNFα secreted from neonatal mouse microglia culture was used. Brains were dissected from P1-P3 NMRI mouse pups, meninges were removed, and brains sliced and washed with Hanks's balanced salt solution (HBSS). Tissue pieces were incubated for approx. 15 min, at 37 °C with 1 mg/mL trypsin in HBSS, and treated with DNaseI (20-40 µg/mL) in 10% FBS + HBSS. Pieces were washed again with HBSS and triturated mechanically. Undissociated tissue was collected by spinning (400 × g, 5 min), followed by another round of mechanical dissociation of the pellet. Dissociated cells were plated in DMEM:F12 (Nutrient Mixture F-12) supplemented with 15% FBS and 0.5% Primocin™ in T-75 cell culture flasks (cat. no. 658175, CELLSTAR®, Greiner Bio-One), an cultivated at 37°C in 5% CO_2 in an air-ventilated humidified incubator. The concentration of FBS was reduced to 10% after 3 d in culture. At least 8 d later, when the cell layer was confluent, microglia were isolated by shaking the plate for 2 h at 37 °C, 190 rpm. Depending on the yield of microglia isolation, 15 000 to 30 000 cells were seeded on clear 48-well plates (ct. no. 677180, CELLSTAR®, Greiner Bio-One) (coated with 0.1 mg/mL poly-L-ornithine). Microglia cells were stimulated by the antagonist TAK-242 (a positive control) and by mitoxantrone, pixantrone and mitoxantrone (2-hydroxyethyl)piperazine 30 min prior the stimulation with LPS (1 ng/mL). For the control wells dimethyl sulfoxide (DMSO) (0.25 ‰) was added, according to the final concentration of DMSO in stimulated wells. After 23 h the media was collected and TNFα levels detected with mouse TNF α ELISA Ready-SET-Go® (cat. no. 88-7324-22, Invitrogen) according to a manufacturer's protocol and measured with Wallac 1420 Victor through absorbance (PerkinElmer). Any effects on cell viability were determined from ATP levels measured with the CellTiter-Glo® as reported above, using Wallac 1420 Victor plate reader.

2.4 Radioligand binding

To demonstrate direct binding to TLR4, the specific binding of tritium-labeled mitoxantrone (Hartmann Analytic GmbH, Braunschweig, Germany) to TLR4-expressing membranes from HEK-Blue™-hTLR4 cell line was investigated. Cells were collected, spinned and frozen down as a pellet at least for 24 h in -80 °C. On the next day, the cells were thawed, suspended in experiment buffer (50 mM phosphate buffer + 1 mM EDTA), and homogenized on ice with ultrasound liquid processors sonicator (Misonix XL-2000) for 5 × 6 s. Nuclei and cell debris were removed by spinning (1000 × g, 10 min, 4 °C), the supernatant was collected and the pellet was resuspended in experiment buffer. The homogenization and spinning were repeated for resuspension, and supernatant collected. The fraction was treated with 10 µg/mL DNaseI and 0.5 mM $MgCl_2$ at room temperature, and once more spinned (10 000 × g, 5 min, 4 °C) to remove mitochondrial DNA. The membrane fraction was collected by ultracentrifuge (100 000 × g, 25 min, 4 °C), and suspended into experiment buffer + 0.32 M saccharose. The fractions were stored in -80 °C. Protein amount was measured by Bradford method (Bradford Reagent, Sigma-Aldrich) according to manufacturer's protocol with bovine serum albumin (BSA) as standard. Five to ten µg protein was used per well diluted in experiment buffer + 1% BSA. Filter-bottomed 96-well MultiScreen HTS plates (Millipore) were used. LPS-RS standard (cat. code tlrl-rslps, InvivoGen), lipopolysaccharide from the photosynthetic bacterium *Rhodobacter sphaeroides* was used as a cold ligand, control for assessing non-specific binding. Excessive amount of LPS-RS (100 ng/mL) was used in order to saturate TLR4 receptors, and thus prevent radio-ligand binding on these receptors. The cold-ligand or an equal volume of experiment buffer was added to wells of unspecific binding or total binding,

respectively, prior loading the membrane fraction samples. After loading the membrane fraction samples, the radio-ligand was added to all wells, and plates were incubated for 2 h at room temperature to reach equilibrium. Plates were washed with cold PBS to remove unbound radio-ligand. Liquid scintillation cocktail Optiphase HiSafe 3 (PerkinElmer) was added, and radioactivity was measured with liquid scintillation counting (CPM) (Wallac Microbeta Trilux microplate liquid scintillation counter, PerkinElmer). Specific binding was determined by subtracting the non-specific binding from total binding. A second method for determining non-specific binding was also tested using membrane fraction from HEK-293T cells that are not expressing TLR4s, and the results found to be highly concordant (supplementary material, Figure S1).

2.5 Statistical analysis

Biological experiments were conducted in triplicate (TNFα detection and binding) or in quadruplicate (SEAP), and using several batches of cells. Data were normalized to maximum before averaging, and presented with mean ± S.E.M (TNFα detection and binding) or mean ± ST.DEV (SEAP). Data were analyzed with Prism 5 and Prism 7 (GraphPad Software Inc. La Jolla, CA, USA), and significance was defined with 2-way ANOVA, followed by Tukey's (SEAP) or Fischer's LSD (TNFα) *post hoc* tests. Significance is marked as follows: ns (not significant; $P > 0.05$), * $P < 0.05$, * * $P < 0.01$, *** $P < 0.001$, **** $P < 0.0001$. Data were visualized with Prism 5, Prism 7, Pymol and Discovery Studio.

3 Results

3.1 Virtual screening

Five independent lists of 200 compounds were constructed totaling 1 000 compounds that could be physically obtained. Controls that could be used to calculate enrichment factors were lacking in virtual screens, since the screens were conducted in near absence of known small-molecule TLR4 antagonists. Thus multiple computational methods were used and combined, with the hope for one to be superior to the others. Since very few hits were obtained after primary experimental screen, it does not make sense to actually compare the virtual screening methods in retrospect.

As a result of the virtual screens, for similarity search, more than 200 most similar compounds to the β-amino alcohol derivative were obtained (Tanimoto similarity above 0.5). For pharmacophore modeling of the MD-2 loop, eight features were defined; and for the pharmacophore modeling of LPS, five features were defined, drawn from molecular interactions seen in the X-ray structure (Park et al., 2009) (**Tables 1** and **2, Figure 2**). Compounds were then retrieved to fit hypotheses combining four out of eight features (MD-2 site) or four out of five features (LPS site). Features (**Figure 2**, labeled with numbers) are defined in detail in **Tables 1** and **2**. The features were selected to keep enough compounds in the hit lists while including the molecular interactions regarded as significant. The active compound identified in this study, mitoxantrone, was originally returned from the LPS pharmacophore-based screen. The docking screens were blindly run in the two structural areas identified (**Figure 3**). Since docking screens simply rank the library, they always return a populated hit list.

3.2 Experimental screening using a gene-reporter assay

The primary screening resulted in a small hit list of 20 compounds showing inhibition of the SEAP LPS-induced activation signal superior to 20%, at least in one replica well (**Figure 5**). The screening was conducted in two replica plates, and when limiting the hit criteria as observation in both replica wells, the hit list contain only 11 compounds: mitoxantrone (**Figure 1**), vatalanib, benazebril, CAS128113-19-9 (5-[[2-(dimethylamino)ethyl]amino]-8-hydroxy-6*H*-[1,2,3]triazolo[4,5,1-*d*,*e*]acridin-6-one), (-)-etoposide, gemcitabine (4-amino-1-[(2*R*,4*R*,5*R*)-3,3-difluoro-4-hydroxy-5-(hydroxymethyl)oxolan-2-yl]pyrimidin-2-one), salicin, CAS1021989-35-4, CAS900453-15-8, foscarnet (phosphonoformic acid), and CAS610281-22-6 (**Figure 4**). Having high well-to-well variability when compared to the controls (only DMSO and DMSO + LPS treated wells), the data was normalized to the local average, which indeed lowered the variation between wells. Controls worked as expected, i.e. the negative control LPS (1 ng/mL) treatment increased the signal by 3.9-fold (70% of maximal); whereas the positive control TAK-242 (500 nM) reduced the LPS-induction down to 20-25%, i.e. showed full inhibition. Only two compounds from the hit list of 11 compounds, mitoxantrone and (-)-etoposide, showed slight cytotoxicity when cell viability was controlled with CellTiter-Glo (74.4% and 78.9%, respectively, of control well ATP representing 100% viable cells). Mitoxantrone was clearly the strongest inhibitor of the list, as cells treated with mitoxantrone (5 µM) were showing only 16.5% of the submaximal signal of LPS-induced SEAP.

Mitoxantrone is a polypharmacological immunosuppressive drug that is mostly used for the treatment of various cancers (Evison et al., 2016) and MS (English and Aloi, 2015). The main limitation of the drug is due to its cardiotoxicity (Pattoneri et al., 2009; Reis-Mendes et al., 2015), and therefore less toxic derivatives have been developed, including pixantrone (Hasinoff et al., 2016) and the mitoxantrone metabolite mitoxantrone (2-hydroxyethyl)piperazine (Reis-Mendes et al., 2017). Mitoxantrone is a well-known inhibitor of topoisomerase II (Tewey et al., 1984), but it

also has various other targets (see for a recent review (Evison et al., 2016)). Despite the well-characterized cardiotoxic mechanism of mitoxantrone, its immunosuppressive mechanism is not fully understood. Lowering the levels of inflammatory cytokines is mostly thought to be derived from preventing proliferation of macrophages, such as T- and B-cells (Maghzi et al., 2011), as well as from preventing the migration of immunocompetent cells (Kopadze et al., 2006). The mechanism of pixantrone has been considered to be similar to mitoxantrone (Mazzanti et al., 2005).

Considering distinctly the best hit, commercially available compounds around the mitoxantrone were searched, and three analogues were included to further tests. As a result of the primary screen, accounting for the commercial availability of the other hits, 11 compounds were chosen to undergo validation: mitoxantrone, banoxantrone, pixantrone, mitoxantrone (2-hydroxyethyl)piperazine, vatalanib, benazepril, (-)-etoposide, salicin, CAS1021989-35-4, CAS900453-15-8 and CAS610281-22-6. Due to commercial unavailability or unwanted properties CAS-128113-19-9, foscarnet and gemcitabine were excluded from the further validation.

3.3 Validation of positive hits

After purchasing compounds from individual suppliers, 11 compounds were retested at three different concentrations (0.5 µM, 1 µM, 5 µM). As a result, only one compound from the primary experimental screen, mitoxantrone, showed significant dose-response-dependent inhibition of TLR4 activation signal (2-way ANOVA, $P \leq 0.0001$) (**Figure 6a**). Mitoxantrone lowered the SEAP levels to 65% ± 1.7% at 1 µM. In addition, the analogues tested, pixantrone (**Figure 6a**) and mitoxantrone (2-hydroxyethyl)piperazine (**Figure 6a**), showed weaker concentration-dependent inhibition, lowering SEAP levels to 71% ± 3.4%; 72% ± 1.8%, respectively, at the same concentration (**Figure 6a**). Together, the activity of the analogues supports the activity of mitoxantrone. Mitoxantrone and analogues showed significant cytotoxicity (2-way ANOVA, $P \leq 0.0001$), at 5 µM, showing approx. 70% of control well ATP; but only mitoxantrone was significantly cytotoxic at lower concentrations, showing approx. 79% of control well ATP (**Figure 6b**). Next, we wanted to exclude the possibility that mitoxantrone and its derivatives reduce SEAP levels in a TLR4-independent manner (e.g. by interfering with other events either downstream or upstream of the reporter gene transcription (Chang et al., 2005)). For that purpose we assessed the effect of these compounds on reporter gene activation by PMA, a specific protein kinase C (PKC) activator (Takeuchi et al., 1992). Mitoxantrone and derivatives showed a significant effect (2-way ANOVA, $P \leq 0.0001$) on PMA-induced activation of the SEAP reporter gene, but not a typical dose-response. Surprisingly, TLR4 bound antagonist TAK-242 (500 nM) also had a significant lowering effect on PMA-induced reporter activation (2-way ANOVA, $P \leq 0.0001$) (**Figure 6c**). Thus, the effect of compounds was compared also to the effect of TAK-242. Only the highest tested concentrations of mitoxantrone and pixantrone (5 µM) had a stronger effect on PMA-induced reporter activation than TAK-242 (Tukey's test, $P \leq 0.0001$; $P \leq 0.05$; respectively), an effect likely caused by the cytotoxicity of these compounds at higher concentration (**Figure 6d**).

3.4 TNFα detection

A concentration-dependent effect of mitoxantrone, pixantrone and mitoxantrone (2-hydroxyethyl)piperazine on LPS-stimulated mice microglia was tested to investigate the effect of the compounds in the production of proinflammatory cytokines. A clear concentration-dependent and significant (2-way ANOVA, $P \leq 0.0001$, followed by Fisher's LSD analysis) effect on TNFα production was seen with pixantrone and mitoxantrone (2-hydroxyethyl)piperazine (**Figure 7**). At 5 µM concentration, pixantrone and mitoxantrone (2-hydroxyethyl)piperazine reduced significantly (Fischer's LSD, $P \leq 0.0001$) the level of TNFα to 46% ± 14.9% and 48% ± 10.1%, respectively, from only LPS-treated cells. A significant effect (Fischer's LSD, $P \leq 0.01$) was seen also at 1 µM,

where compounds lowered TNFα levels to 67% (± 11.4% [pixantrone]; ± 9% [mitoxantrone (2-hydroxyethyl)piperazine]). The positive control TAK-242 (500nM) lowered TNFα levels to 34.3% ± 0.1%. However, significant cytotoxicity (2-way ANOVA, $P \leq 0.05$) was observed. At the highest concentration (5 µM) of pixantrone and mitoxantrone (2-hydroxyethyl)piperazine lowered the ATP levels to ~79% of ATP of LPS-treated cells, however the effect was significant (Fischer's LSD, $P \leq 0.05$) only in pixantrone-treated cells. Mitoxantrone showed high cytotoxicity on microglia (500 nM lowered ATP levels to 14.6% ± 2.3%; N=2), and thus TNFα levels could not be analyzed (supplementary material, Figure S2). At low toxic concentration (50 nM), mitoxantrone reduced the TNFα production from only LPS-treated cells around the same range than its derivatives (84.5% ± 20.8%; N=2; supplementary material, Figure S3).

3.5 Radioligand binding

To demonstrate the action of mitoxantrone through the TLR4 receptor, we measured the binding of [^{3}H]mitoxantrone to TLR4-expressing membrane fraction from HEK-Blue™-hTLR4 cells in the presence or absence of a known TLR4 antagonist LPS-RS. The presence of LPS-RS (at final concentration of 100 ng/mL) reduced the binding of [^{3}H]mitoxantrone to membrane fraction of HEK-Blue™-hTLR4 cells, but did not have an effect on [^{3}H]mitoxantrone binding to membrane fraction of HEK-293T cells that do not express TLR4 (supplementary material, Figure S4).

At lower concentrations (≤ 125 nM) the concentration-response curve seems to reach the saturation, however at higher concentrations the response ascends steeply (**Figure 8**). This is likely caused by high non-specific binding, especially seen at high concentrations (supplementary material, Figure S5). However, the LPS-RS-sensitive TLR4-specific binding was observed concentration-dependently and robustly in several repeats at many concentrations of [^{3}H]mitoxantrone (**Figure 8**). At higher concentrations, non-specific binding partially occluded the results: high variation in binding experiments was observed and saturation was not distinctly reached, most likely due to high non-specific binding, binding affinity values could not be determined reliably. The fact that specific binding was observed, when the cold ligand LPS-RS was present, may suggest that [^{3}H]mitoxantrone binds to the same site as lipopolysaccharides.

4 Discussion

Taken together, results of this study suggest that mitoxantrone and its derivatives pixantrone and mitoxantrone (2-hydroxyethyl)piperazine inhibit the TLR4 activation signal by binding directly to TLR4 and most likely at the same binding site as LPS. This data adds to the emerging number of novel small molecule inhibitors of TLR4 that have been reported recently (see e.g. (Marshall et al., 2016; Peri and Calabrese, 2014; Wang et al., 2016; Zaffaroni and Peri, 2018). These various TLR4 ligands are from synthetic origin are such as neoseptins and Ugi compounds, and several are lipid mimetics of the glycolipid part of LPS; or from natural sources such as curcumin, cinnamaldehyde and glycyrrhizin.

The inhibitory effect of mitoxantrone, pixantrone, and mitoxantrone (2-hydroxyethyl)piperazine on TLR4 activation signal in SEAP-reporter assay was detected. The effect was significant and concentration-dependent, and not mediated through cytotoxicity (controlled by ATP counts) at lower concentrations. However, an issue with reporter assays is often having the reporter far downstream from the target, thus the mechanism of action may be indirect from the target and not occurring through target activation. Thus, a possible TLR4-independent effect in SEAP-reporter assay was investigated with PMA-induction of NF-κB. A significant, but not distinctly concentration-dependent, effect on PMA-induction was observed, indicating that the reducing effect of the compounds on LPS-driven activation signal is likely not a TLR4-independent effect on the NF-κB activation pathway. Moreover, the effect of mitoxantrone and derivatives was not significantly higher than the effect of the control antagonist TAK-242 on PMA-induced TLR4 activation at lower concentrations (≤ 1 μM).

Further, [^{3}H]mitoxantrone binds to the membrane fraction of TLR4-expressing cells. However, it is still possible that the compounds would bind to membrane-anchored adaptor proteins in the membrane fraction and not to TLR4. In addition, a large variation in bound molecule per milligram of protein between experiments, affected the robustness of the binding results. However, all the experiments showed concentration-dependent specific binding when controlled with LPS-RS (or with HEK-293T membrane fraction). Being able to block [^{3}H]mitoxantrone binding sites with LPS-RS suggests a common binding site, likely in TLR4. However, to definitely prove specificity, a counter screen with other TLRs would be needed, which is beyond the scope of this study.

There is previous evidence, that mitoxantrone is actually rather indirect promoter of activation of NF-κB through topoisomerase II poisoning, in leukemia HL60 cells (but not HL60/MX2 cells that do not express topoisomerase II), and NF-κB is also known as one of the apoptosis regulators (Boland et al., 2000). There is also opposite evidence of mitoxantrone being potent inhibitor of PKC (Takeuchi et al., 1992), with 8.5 μM IC_{50} value in HL60 cells, which inhibits further NF-κB. The inhibition was mostly detected in cytosolic fraction. Cytosolic fraction was ruled out in our binding measurements, indicating that mechanisms of inhibition are not only direct to PKC, but include TLR4-dependent activation too. This could partly, in addition to cytotoxicity, also explain significant inhibition of mitoxantrone and analogues (5 μM) on PMA induction.

An immunosuppressive/modulatory mechanism of mitoxantrone has been described in the periphery, showing the inhibitory effect on proliferation and migration of macrophages (Kopadze et al., 2006; Maghzi et al., 2011), as well as showing a cytotoxic and immunomodulatory effect on CNS-specific macrophages (microglia) (Li et al., 2012). However, no protein molecular target has been described before this study. The data presented here indicate that the mechanism could be TLR4-mediated. Consistent with previous data on mitoxantrone (Fidler et al., 1986; Neuhaus et al., 2001) and pixantrone (Mazzanti et al., 2005), a concentration-dependent and significant reduction

of TNFα is here detected and reported to the best of our knowledge for the first time in mouse microglia using pixantrone and mitoxantrone (2-hydroxyethyl)piperazine-treated cells.

5 Conclusion

Toll-like receptor 4 is a very challenging protein for *in silico* screens due to its large size and location at an interaction hub as well as to the presence of multiple potential binding sites. Our *in vitro* tests lead to a very small hit rate, with only one hit eventually, which is much lower than for example G protein-coupled transporters or ABC transporters (Turku et al., 2016; Wissel et al., 2015). The absence of a well-identified binding pocket as well as the scarcity of the known ligands to be used as controls has certainly significantly hampered the virtual screens.

Nonetheless, this study suggests new potential mechanisms of action for mitoxantrone by implying that its immunosuppressive effect is TLR4-dependent. Due to the fact that mitoxantrone and its derivatives are promiscuous drugs, it is difficult to evaluate their therapeutic potential when targeting TLR4. In addition, intravenously administered mitoxantrone or analogues do not cross the blood-brain-barrier prominently. Thus, TLR4-mediated effects in the CNS are unlikely unless the blood-brain barrier is disrupted which may be the case e.g. in MS (Ergin et al., 2012). Regardless of such, the scaffold of mitoxantrone could be useful in the design of novel TLR4 inhibitors.

Author_statement

Maiju Rinne: Conceptualization; Data curation; Formal analysis; Investigation; Methodology;; Supervision; Validation; Visualization; Roles/Writing - original draft; Writing - review & editing.

Kert Mätlik: Conceptualization; Data curation; Formal analysis; Investigation; Methodology;; Supervision; Writing - review & editing.

Tiina Ahonen: Formal analysis; Validation; Writing - review & editing.

Fabio Vedovi: Conceptualization; Data curation; Formal analysis; Visualization; Roles/Writing - original draft; Writing - review & editing.

Giovanni Zappia: Conceptualization; Funding acquisition; Supervision; Writing - review & editing.

Vânia M. Moreira: Conceptualization; Funding acquisition; Supervision; Writing - review & editing.

Jari Yli-Kauhaluoma: Conceptualization; Funding acquisition; Project administration; Supervision; Writing - review & editing.

Sakari Leino: Formal analysis; Investigation; Visualization; Writing - review & editing.

Outi Salminen: Formal analysis; Investigation; Visualization; Writing - review & editing.

Eija Kalso: Conceptualization; Funding acquisition; Project administration; Supervision; Writing - review & editing.

Mikko Airavaara: Conceptualization; Funding acquisition; Investigation; Methodology; Project administration; Resources; Supervision; Visualization; Roles/Writing - original draft; Writing - review & editing.

Henri Xhaard: Conceptualization; Funding acquisition; Investigation; Methodology; Project administration; Resources; Supervision; Visualization; Roles/Writing - original draft; Writing - review & editing.

Data Availability Statement

All data analyzed during this study are included in this published article. Other raw data will be made accessible upon reasonable request.

Ethics Statement

Experimental procedures were approved by the National Animal Experiment Board of Finland (protocol approval number ESAVI/7812/04.10.07/2015) and followed local laws and regulations.

Funding

This work was supported by the European Union Seventh Framework Programme (FP7/2007 - 2013) under grant agreement no 602919 (GLORIA) and by Business Finland (Finnish Funding Agency for Innovation, Tekes, 3iRegeneration, Project 40395/13). MA was also funded by Academy of Finland grant 250275.

Acknowledgements

Mari Heikkinen, Congjun Zheng are gratefully acknowledged for technical assistance with the experiments. CSC – IT Center for Science is thanked for organizing national infrastructure in computational chemistry. The Drug Discovery and Chemical Biology (DDCB) Biocenter Finland consortium is acknowledged for organizing computational resources in the H.X. group, DDCB is also thanked, especially Dr. Jani Saarela and Dr Laura Turunen, for setting up the High Throughput Biomedicine unit (HTB) that provided the screening facilities and compound collection used in this manuscript. The MuTaLig COST action 15135 is thanked for setting up a network around poly-pharmacology.

6 References

Akira, S., Uematsu, S., Takeuchi, O., 2006. Pathogen Recognition and Innate Immunity. Cell 124, 783–801. https://doi.org/10.1016/J.CELL.2006.02.015

Akira, S., Yamamoto, M., Takeda, K., 2003. Role of adapters in Toll-like receptor signalling. Biochem. Soc. Trans. 31, 637–42. https://doi.org/10.1042/

Andersson, Å., Covacu, R., Sunnemark, D., Danilov, A.I., Dal Bianco, A., Khademi, M., Wallström, E., Lobell, A., Brundin, L., Lassmann, H., Harris, R.A., 2008. Pivotal Advance: HMGB1 expression in active lesions of human and experimental multiple sclerosis. J. Leukoc. Biol. 84, 1248–1255. https://doi.org/10.1189/jlb.1207844

Baell, J.B., Nissink, J.W.M., 2018. Seven Year Itch: Pan-Assay Interference Compounds (PAINS) in 2017—Utility and Limitations. ACS Chem. Biol. 13, 36–44. https://doi.org/10.1021/acschembio.7b00903

Baeuerle, P.A., Henkel, T., 1994. Function and Activation of NF-kappaB in the Immune System. Annu. Rev. Immunol. 12, 141–179. https://doi.org/10.1146/annurev.iy.12.040194.001041

Bevan, D.E., Martinko, A.J., Loram, L.C., Stahl, J.A., Taylor, E.R., Joshee, S., Watkins, L.R., Yin, H., 2010. Selection, Preparation, and Evaluation of Small- Molecule Inhibitors of Toll-Like Receptor 4. ACS Med. Chem. Lett. 1, 194–198. https://doi.org/10.1021/ml100041f

BIOvIA, D.S., 2015. Discovery studio modeling environment, San Diego, Dassault Syst.

Boland, M.P., Fitzgerald, K.A., O'Neill, L.A., 2000. Topoisomerase II is required for mitoxantrone to signal nuclear factor kappa B activation in HL60 cells. J. Biol. Chem. 275, 25231–8.

Chang, M.-S., Chen, B.-C., Yu, M.-T., Sheu, J.-R., Chen, T.-F., Lin, C.-H., 2005. Phorbol 12-myristate 13-acetate upregulates cyclooxygenase-2 expression in human pulmonary epithelial cells via Ras, Raf-1, ERK, and NF-κB, but not p38 MAPK, pathways. Cell. Signal. 17, 299–310. https://doi.org/10.1016/j.cellsig.2004.07.008

Chavez, S.A., Martinko, A.J., Lau, C., Pham, M.N., Cheng, K., Bevan, D.E., Mollnes, T.E., Yin, H., 2011. Development of β-Amino Alcohol Derivatives That Inhibit Toll-like Receptor 4 Mediated Inflammatory Response as Potential Antiseptics. J. Med. Chem. 54, 4659–4669. https://doi.org/10.1021/jm2003365

English, C., Aloi, J.J., 2015. New FDA-Approved Disease-Modifying Therapies for Multiple Sclerosis. Clin. Ther. 37, 691–715. https://doi.org/10.1016/j.clinthera.2015.03.001

Ergin, A., Wang, M., Zhang, J., Bigio, I., Joshi, S., 2012. Noninvasive in vivo optical assessment of blood brain barrier permeability and brain tissue drug deposition in rabbits. J. Biomed. Opt. 17, 057008. https://doi.org/10.1117/1.JBO.17.5.057008

Evison, B.J., Sleebs, B.E., Watson, K.G., Phillips, D.R., Cutts, S.M., 2016. Mitoxantrone, More than Just Another Topoisomerase II Poison. Med. Res. Rev. 36, 248–299. https://doi.org/10.1002/med.21364

Fidler, J.M., DeJoy, S.Q., Smith, F.R., Gibbons, J.J., 1986. Selective immunomodulation by the antineoplastic agent mitoxantrone. II. Nonspecific adherent suppressor cells derived from

mitoxantrone-treated mice. J. Immunol. 136, 2747–54.

Grace, P.M., Rolan, P.E., Hutchinson, M.R., 2011. Peripheral immune contributions to the maintenance of central glial activation underlying neuropathic pain. Brain. Behav. Immun. 25, 1322–1332. https://doi.org/10.1016/J.BBI.2011.04.003

Hasinoff, B.B., Wu, X., Patel, D., Kanagasabai, R., Karmahapatra, S., Yalowich, J.C., 2016. Mechanisms of Action and Reduced Cardiotoxicity of Pixantrone; a Topoisomerase II Targeting Agent with Cellular Selectivity for the Topoisomerase II Isoform. J. Pharmacol. Exp. Ther. 356, 397–409. https://doi.org/10.1124/jpet.115.228650

Hyakkoku, K., Hamanaka, J., Tsuruma, K., Shimazawa, M., Tanaka, H., Uematsu, S., Akira, S., Inagaki, N., Nagai, H., Hara, H., 2010. Toll-like receptor 4 (TLR4), but not TLR3 or TLR9, knock-out mice have neuroprotective effects against focal cerebral ischemia. Neuroscience 171, 258–267. https://doi.org/10.1016/j.neuroscience.2010.08.054

Jacobs, T., 2005. No pain, no gain? Nat. Biotechnol. 23, 934–934. https://doi.org/10.1038/nbt0805-934

Janssens, S., Beyaert, R., 2003. Role of Toll-like receptors in pathogen recognition. Clin. Microbiol. Rev. 16, 637–46.

Jeannin, P., Jaillon, S., Delneste, Y., 2008. Pattern recognition receptors in the immune response against dying cells. Curr. Opin. Immunol. 20, 530–537. https://doi.org/10.1016/j.coi.2008.04.013

Kanzler, H., Barrat, F.J., Hessel, E.M., Coffman, R.L., 2007. Therapeutic targeting of innate immunity with Toll-like receptor agonists and antagonists. Nat. Med. 13, 552–9. https://doi.org/10.1038/nm1589

Kawai, T., Akira, S., 2009. The roles of TLRs, RLRs and NLRs in pathogen recognition. Int. Immunol. 21, 317–337. https://doi.org/10.1093/intimm/dxp017

Kopadze, T., Dehmel, T., Hartung, H.-P., Stüve, O., Kieseier, B.C., 2006. Inhibition by Mitoxantrone of In Vitro Migration of Immunocompetent Cells. Arch. Neurol. 63, 1572. https://doi.org/10.1001/archneur.63.11.1572

Kroner, A., Vogel, F., Kolb-Mäurer, A., Kruse, N., Toyka, K.V., Hemmer, B., Rieckmann, P., Mäurer, M., 2005. Impact of the Asp299Gly polymorphism in the toll-like receptor 4 (tlr-4) gene on disease course of multiple sclerosis. J. Neuroimmunol. 165, 161–165. https://doi.org/10.1016/j.jneuroim.2005.03.012

Kuang, X., Huang, Y., Gu, H.-F., Zu, X.-Y., Zou, W.-Y., Song, Z.-B., Guo, Q.-L., 2012. Effects of intrathecal epigallocatechin gallate, an inhibitor of Toll-like receptor 4, on chronic neuropathic pain in rats. Eur. J. Pharmacol. 676, 51–6. https://doi.org/10.1016/j.ejphar.2011.11.037

Li, J.-M., Yang, Y., Zhu, P., Zheng, F., Gong, F.-L., Mei, Y.-W., 2012. Mitoxantrone exerts both cytotoxic and immunoregulatory effects on activated microglial cells. Immunopharmacol. Immunotoxicol. 34, 36–41. https://doi.org/10.3109/08923973.2011.572890

Liu, T., Gao, Y.-J., Ji, R.-R., 2012. Emerging role of Toll-like receptors in the control of pain and itch. Neurosci. Bull. 28, 131–144. https://doi.org/10.1007/s12264-012-1219-5

Lu, Y.-C., Yeh, W.-C., Ohashi, P.S., 2008. LPS/TLR4 signal transduction pathway. Cytokine 42, 145–151. https://doi.org/10.1016/J.CYTO.2008.01.006

Maciejewska Rodrigues, H., Jüngel, A., Gay, R.E., Gay, S., 2009. Innate immunity, epigenetics and autoimmunity in rheumatoid arthritis. Mol. Immunol. 47, 12–18. https://doi.org/10.1016/J.MOLIMM.2009.01.010

Maghzi, A.-H., Borazanci, A., McGee, J., Steven Alexander, J., Gonzalez-Toledo, E., 2011. Multiple Sclerosis: Pathophysiology, Clinical Features, Diagnosis, and Management. Neuroinflammation 1–23. https://doi.org/10.1016/B978-0-12-384913-7.00001-0

Marshall, J.D., Heeke, D.S., Rao, E., Maynard, S.K., Hornigold, D., McCrae, C., Fraser, N., Tovchigrechko, A., Yu, L., Williams, N., King, S., Cooper, M.E., Hajjar, A.M., Woo, J.C., 2016. A Novel Class of Small Molecule Agonists with Preference for Human over Mouse TLR4 Activation. PLoS One 11, e0164632.

Matsunaga, N., Tsuchimori, N., Matsumoto, T., Ii, M., 2011. TAK-242 (resatorvid), a small-molecule inhibitor of Toll-like receptor (TLR) 4 signaling, binds selectively to TLR4 and interferes with interactions between TLR4 and its adaptor molecules. Mol. Pharmacol. 79, 34–41. https://doi.org/10.1124/mol.110.068064

Mattioli, T.A., Leduc-Pessah, H., Skelhorne-Gross, G., Nicol, C.J.B., Milne, B., Trang, T., Cahill, C.M., 2014. Toll-Like Receptor 4 Mutant and Null Mice Retain Morphine-Induced Tolerance, Hyperalgesia, and Physical Dependence. PLoS One 9, e97361. https://doi.org/10.1371/journal.pone.0097361

Mazzanti, B., Biagioli, T., Aldinucci, A., Cavaletti, G., Cavalletti, E., Oggioni, N., Frigo, M., Rota, S., Tagliabue, E., Ballerini, C., Massacesi, L., Riccio, P., Lolli, F., 2005. Effects of pixantrone on immune-cell function in the course of acute rat experimental allergic encephalomyelitis. J. Neuroimmunol. 168, 111–117. https://doi.org/10.1016/J.JNEUROIM.2005.07.010

Meller, S.T., Dykstra, C., Grzybycki, D., Murphy, S., Gebhart, G.F., 1994. The possible role of glia in nociceptive processing and hyperalgesia in the spinal cord of the rat. Neuropharmacology 33, 1471–1478. https://doi.org/10.1016/0028-3908(94)90051-5

Meng, J., Lien, E., Golenbock, D.T., 2010. MD-2-mediated Ionic Interactions between Lipid A and TLR4 Are Essential for Receptor Activation. J. Biol. Chem. 285, 8695–8702. https://doi.org/10.1074/jbc.M109.075127

Milligan, E.D., Watkins, L.R., 2009. Pathological and protective roles of glia in chronic pain. Nat. Rev. Neurosci. 10, 23–36. https://doi.org/10.1038/nrn2533

Miranda-Hernandez, S., Baxter, A.G., 2013. Role of toll-like receptors in multiple sclerosis. Am. J. Clin. Exp. Immunol. 2, 75–93.

Mullarkey, M., Rose, J.R., Bristol, J., Kawata, T., Kimura, A., Kobayashi, S., Przetak, M., Chow, J., Gusovsky, F., Christ, W.J., Rossignol, D.P., 2002. Inhibition of Endotoxin Response by E5564, a Novel Toll-Like Receptor 4-Directed Endotoxin Antagonist. J. Pharmacol. Exp. Ther. 304, 1093–1102. https://doi.org/10.1124/jpet.102.044487

Neuhaus, O., Farina, C., Wekerle, H., Hohlfeld, R., 2001. Mechanisms of action of glatiramer acetate in multiple sclerosis. Neurology 56, 702–8.

https://doi.org/10.1212/wnl.63.12_suppl_6.s15

Nicotra, L., Loram, L.C., Watkins, L.R., Hutchinson, M.R., 2012. Toll-like receptors in chronic pain. Exp. Neurol. 234, 316–329.

O'Brien, K., Fitzgerald, D.C., Naiken, K., Alugupalli, K.R., Rostami, A.M., Gran, B., 2008. Role of the innate immune system in autoimmune inflammatory demyelination. Curr. Med. Chem. 15, 1105–15.

Oblak, A., Jerala, R., 2011. Toll-Like Receptor 4 Activation in Cancer Progression and Therapy. Clin. Dev. Immunol. 2011, 1–12. https://doi.org/10.1155/2011/609579

Ohto, U., Fukase, K., Miyake, K., Shimizu, T., 2012. Structural basis of species-specific endotoxin sensing by innate immune receptor TLR4/MD-2. Proc. Natl. Acad. Sci. U. S. A. 109, 7421–6. https://doi.org/10.1073/pnas.1201193109

Opal, S.M., Laterre, P.-F., Francois, B., LaRosa, S.P., Angus, D.C., Mira, J.-P., Wittebole, X., Dugernier, T., Perrotin, D., Tidswell, M., Jauregui, L., Krell, K., Pachl, J., Takahashi, T., Peckelsen, C., Cordasco, E., Chang, C.-S., Oeyen, S., Aikawa, N., Maruyama, T., Schein, R., Kalil, A.C., Van Nuffelen, M., Lynn, M., Rossignol, D.P., Gogate, J., Roberts, M.B., Wheeler, J.L., Vincent, J.-L., ACCESS Study Group, for the, 2013. Effect of Eritoran, an Antagonist of MD2-TLR4, on Mortality in Patients With Severe Sepsis. JAMA 309, 1154. https://doi.org/10.1001/jama.2013.2194

Park, B.S., Song, D.H., Kim, H.M., Choi, B.-S., Lee, H., Lee, J.-O., 2009. The structural basis of lipopolysaccharide recognition by the TLR4-MD-2 complex. Nature 458, 1191–5. https://doi.org/10.1038/nature07830

Pattoneri, P., Sozzi, F., Pelà, G., Montanari, E., Moruzzi, P., Borghetti, A., Cappellini, M.D., 2009. Assessment of Mitoxantrone-Induced Cardiotoxicity in Patients with Multiple Sclerosis: A Tissue Doppler Echocardiographic Analysis. Echocardiography 26, 397–402. https://doi.org/10.1111/j.1540-8175.2008.00812.x

Peri, F., Calabrese, V., 2014. Toll-like Receptor 4 (TLR4) Modulation by Synthetic and Natural Compounds: An Update. J. Med. Chem. 57, 3612–3622. https://doi.org/10.1021/jm401006s

Peri, F., Piazza, M., 2012. Therapeutic targeting of innate immunity with Toll-like receptor 4 (TLR4) antagonists. Biotechnol. Adv. 30, 251–260. https://doi.org/10.1016/j.biotechadv.2011.05.014

PyMOL 1.7.0.0 Schrödinger, n.d. The PyMOL Molecular Graphics System, Version 1.7.0.0 Schrödinger, LLC.

Reindl, M., Lutterotti, A., Ingram, J., Schanda, K., Gassner, C., Deisenhammer, F., Berger, T., Lorenz, E., 2003. Mutations in the gene for toll-like receptor 4 and multiple sclerosis. Tissue Antigens 61, 85–8.

Reis-Mendes, A., Gomes, A.S., Carvalho, R.A., Carvalho, F., Remião, F., Pinto, M., Bastos, M.L., Sousa, E., Costa, V.M., 2017. Naphthoquinoxaline metabolite of mitoxantrone is less cardiotoxic than the parent compound and it can be a more cardiosafe drug in anticancer therapy. Arch. Toxicol. 91, 1871–1890. https://doi.org/10.1007/s00204-016-1839-z

Reis-Mendes, A.F., Sousa, E., de Lourdes Bastos, M., Costa, V.M., 2015. The Role of the Metabolism of Anticancer Drugs in Their Induced-Cardiotoxicity. Curr. Drug Metab. 17, 75–90.

Rice, T.W., Wheeler, A.P., Bernard, G.R., Vincent, J.-L., Angus, D.C., Aikawa, N., Demeyer, I., Sainati, S., Amlot, N., Cao, C., Ii, M., Matsuda, H., Mouri, K., Cohen, J., 2010. A randomized, double-blind, placebo-controlled trial of TAK-242 for the treatment of severe sepsis. Crit. Care Med. 38, 1685–94. https://doi.org/10.1097/CCM.0b013e3181e7c5c9

Rishton, G.M., 1997. Reactive compounds and in vitro false positives in HTS. Drug Discov. Today 2, 382–384. https://doi.org/10.1016/S1359-6446(97)01083-0

Rock, F.L., Hardiman, G., Timans, J.C., Kastelein, R.A., Bazan, J.F., 1998. A family of human receptors structurally related to Drosophila Toll. Proc. Natl. Acad. Sci. U. S. A. 95, 588–93.

Schrödinger Release 2015-3: Maestro, Version 10.3, Schrödinger, LLC, New York, NY., 2015.

Scior, T., Lozano-Aponte, J., Figueroa-Vazquez, V., Yunes-Rojas, J.A., Zähringer, U., Alexander, C., 2013. Three-dimensional mapping of differential amino acids of human, murine, canine and equine TLR4/MD-2 receptor complexes conferring endotoxic activation by lipid A, antagonism by Eritoran and species-dependent activities of Lipid IVA in the mammalian LPS sensor system. Comput. Struct. Biotechnol. J. 7, e201305003. https://doi.org/10.5936/csbj.201305003

Sommer, C., Petrausch, S., Lindenlaub, T., Toyka, K. V, 1999. Neutralizing antibodies to interleukin 1-receptor reduce pain associated behavior in mice with experimental neuropathy. Neurosci. Lett. 270, 25–8.

Sorge, R.E., LaCroix-Fralish, M.L., Tuttle, A.H., Sotocinal, S.G., Austin, J.-S., Ritchie, J., Chanda, M.L., Graham, A.C., Topham, L., Beggs, S., Salter, M.W., Mogil, J.S., 2011. Spinal Cord Toll-Like Receptor 4 Mediates Inflammatory and Neuropathic Hypersensitivity in Male But Not Female Mice. J. Neurosci. 31, 15450–15454. https://doi.org/10.1523/JNEUROSCI.3859-11.2011

Takashima, K., Matsunaga, N., Yoshimatsu, M., Hazeki, K., Kaisho, T., Uekata, M., Hazeki, O., Akira, S., Iizawa, Y., Ii, M., 2009. Analysis of binding site for the novel small-molecule TLR4 signal transduction inhibitor TAK-242 and its therapeutic effect on mouse sepsis model. Br. J. Pharmacol. 157, 1250–1262. https://doi.org/10.1111/j.1476-5381.2009.00297.x

Takeuchi, N., Nakamura, T., Takeuchi, F., Hashimoto, E., Yamamura, H., 1992. Inhibitory effect of mitoxantrone on activity of protein kinase C and growth of HL60 cells. J. Biochem. 112, 762–767. https://doi.org/10.1093/oxfordjournals.jbchem.a123972

Tang, S.-C., Arumugam, T. V., Xu, X., Cheng, A., Mughal, M.R., Jo, D.G., Lathia, J.D., Siler, D.A., Chigurupati, S., Ouyang, X., Magnus, T., Camandola, S., Mattson, M.P., 2007. Pivotal role for neuronal Toll-like receptors in ischemic brain injury and functional deficits. Proc. Natl. Acad. Sci. 104, 13798–13803. https://doi.org/10.1073/pnas.0702553104

Tanga, F.Y., Nutile-McMenemy, N., DeLeo, J.A., 2005. The CNS role of Toll-like receptor 4 in innate neuroimmunity and painful neuropathy. Proc. Natl. Acad. Sci. U. S. A. 102, 5856–61. https://doi.org/10.1073/pnas.0501634102

Tewey, K.M., Rowe, T.C., Yang, L., Halligan, B.D., Liu, L.-F., 1984. Adriamycin-induced DNA damage mediated by mammalian DNA topoisomerase II. Science (80-.). 226, 466–468.

Turku, A., Borrel, A., Leino, T.O., Karhu, L., Kukkonen, J.P., Xhaard, H., 2016. Pharmacophore Model To Discover OX_1 and OX_2 Orexin Receptor Ligands. J. Med. Chem. 59, 8263–8275. https://doi.org/10.1021/acs.jmedchem.6b00333

Vaure, C., Liu, Y., 2014. A comparative review of toll-like receptor 4 expression and functionality in different animal species. Front. Immunol. 5, 316. https://doi.org/10.3389/fimmu.2014.00316

Wang, Y., Su, L., Morin, M.D., Jones, B.T., Whitby, L.R., Surakattula, M.M.R.P., Huang, H., Shi, H., Choi, J.H., Wang, K., Moresco, E.M.Y., Berger, M., Zhan, X., Zhang, H., Boger, D.L., Beutler, B., 2016. TLR4/MD-2 activation by a synthetic agonist with no similarity to LPS. Proc. Natl. Acad. Sci. 113, E884 LP-E893. https://doi.org/10.1073/pnas.1525639113

Watkins, L.., Martin, D., Ulrich, P., Tracey, K.., Maier, S.., 1997. Evidence for the involvement of spinal cord glia in subcutaneous formalin induced hyperalgesia in the rat. Pain 71, 225–235. https://doi.org/10.1016/S0304-3959(97)03369-1

Willett, P., 2003. Similarity-based approaches to virtual screening. Biochem. Soc. Trans. 31, 603–6. https://doi.org/10.1042/

Wissel, G., Kudryavtsev, P., Ghemtio, L., Tammela, P., Wipf, P., Yliperttula, M., Finel, M., Urtti, A., Kidron, H., Xhaard, H., 2015. Exploring the structure–activity relationships of ABCC2 modulators using a screening approach. Bioorg. Med. Chem. 23, 3513–3525. https://doi.org/10.1016/j.bmc.2015.04.029

Wu, F., Bian, J., Miao, X., Huang, S., Xu, X., Gong, D., Sun, Y., Lu, Z., Yu, W., 2010. Intrathecal siRNA against Toll-like receptor 4 reduces nociception in a rat model of neuropathic pain. Int. J. Med. Sci. 7, 251–9.

Wu, Z., Wang, S., Wu, I., Mata, M., Fink, D.J., 2015. Activation of TLR-4 to produce tumour necrosis factor-α in neuropathic pain caused by paclitaxel. Eur. J. Pain 19, 889–898. https://doi.org/10.1002/ejp.613

Zaffaroni, L., Peri, F., 2018. Recent advances on Toll-like receptor 4 modulation: new therapeutic perspectives. Future Med. Chem. 10, 461–476. https://doi.org/10.4155/fmc-2017-0172

Zhou, D., Zhuang, Y., Chen, W., Li, W., Miao, B., 2018. Effects of Duloxetine on the Toll-Like Receptor 4 Signaling Pathway in Spinal Dorsal Horn in a Rat Model of Diabetic Neuropathic Pain. Pain Med. 19, 580–588. https://doi.org/10.1093/pm/pnx125

Figure Captions

Figure 1. Chemical structures of the antineoplastic agents mitoxantrone, pixantrone, and mitoxantrone (2-hydroxyethyl)piperazine, TAK-242 and a racemic β-amino alcohol derivative (Bevan et al., 2010) used in similarity search.

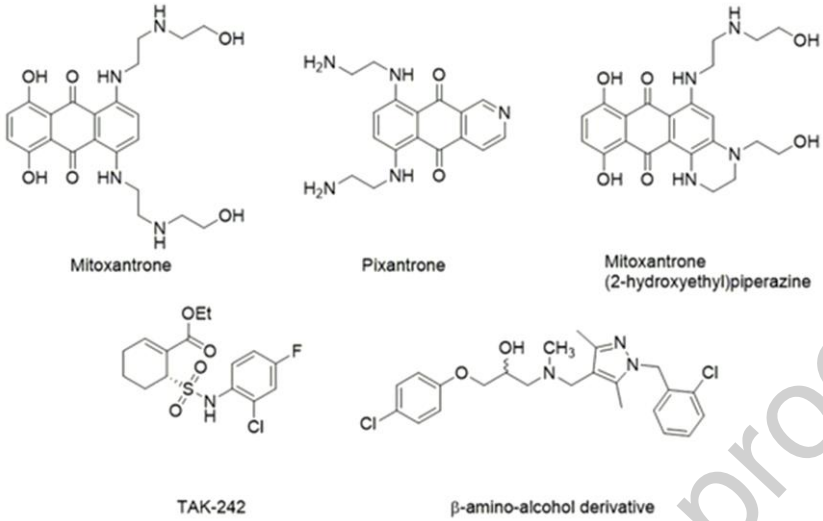

Figure 2. Pharmacophore features based on (a) MD-2 loop, from Gly-97 to Leu-108, and (b) LPS binding modes. Green = hydrogen bond acceptor, magenta = hydrogen bond donor, and blue = ionic interaction to TLR4.

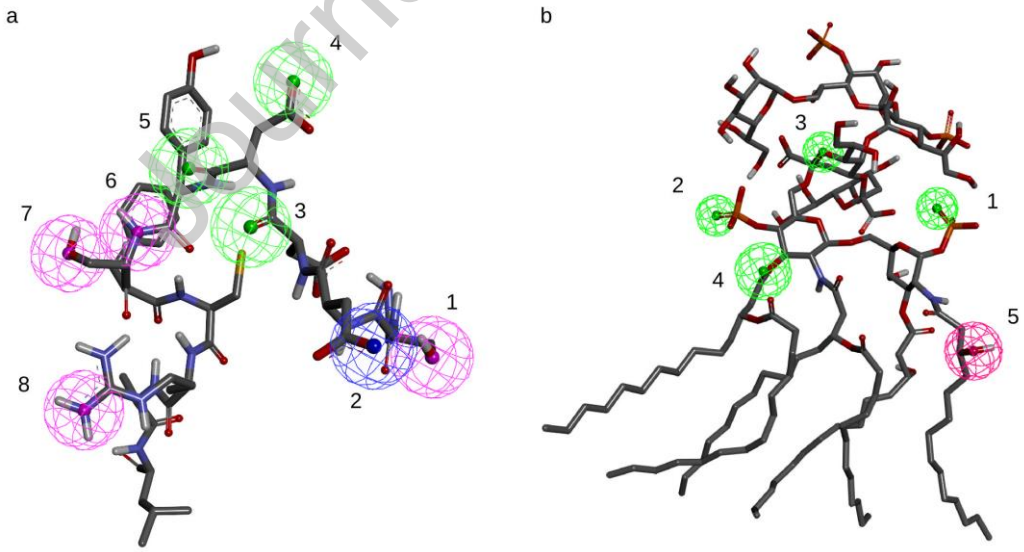

Figure 3. (a) Extracellular domain of human TLR4 dimer (green), in complex with MD-2 helper protein (magenta) and co-ligand lipopolysaccharide (cyan) (b) MD-2 loop F126 (magenta) binding site and interactions with TLR4 (green). (c) LPS (cyan) binding site and key interactions of glycolipid part with TLR4 (green), and the second TLR4 monomer (blue*).

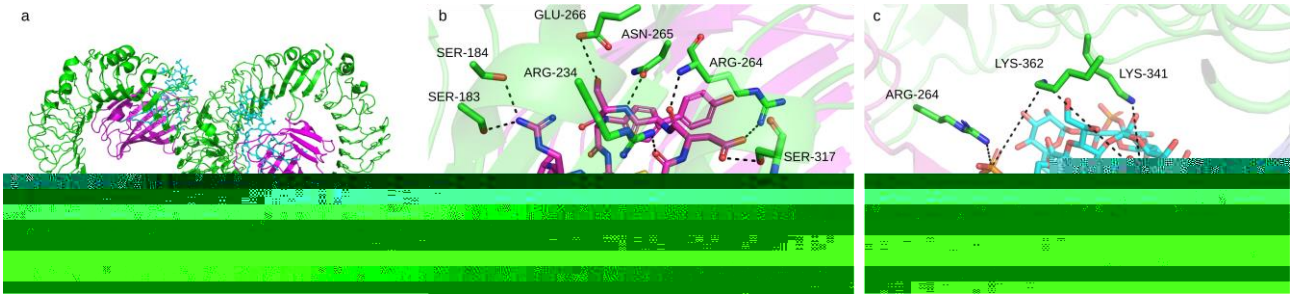

Figure 4. Chemical structures of banoxantrone, vatalanib, benazepril, (-)-etoposide, salicin, CAS 1021989-35-4, CAS 900453-15-8, and CAS 610281-22-6.

Figure 5. (a) Results of the experimental screening of 1000 compounds, replica wells plotted to proprietary axis. Compounds showing > 20% inhibition of full-activation of LPS induction in both replica wells are circled with red. (b) Twenty best hits of the first round of experimental screening, showing inhibition of LPS-induced activation signal > 20% at least in one replica well. a) Mitoxantrone, b) vatalanib, c) benazebril, d) CAS128113-19-9, e) (-)-etoposide, f) gemcitabine, g) salicin, h) CAS1021989-35-4, i) CAS900453-15-8, j) foscarnet, k) CAS610281-22-6 inhibited LPS-induced activation signal ≥ 20% (average). Compounds l-t were not added to further validation, because of their low inhibition potential (average < 20%). Data normalized to local average.

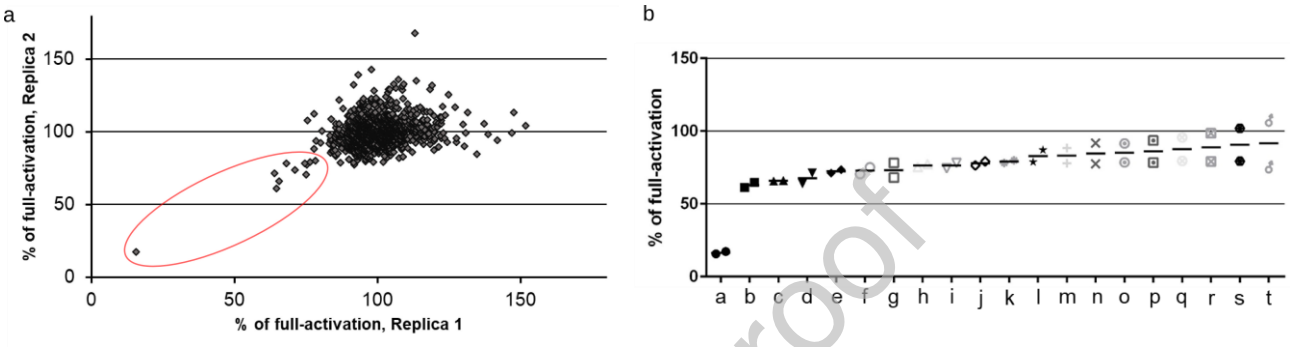

Figure 6. Concentration-response on SEAP and cytotoxicity of mitoxantrone, pixantrone and mitoxantrone (2-hydroxyethyl)piperazine. Data normalized to the signal of LPS/PMA treated cells (100%; bar not shown). (a) Inhibitory effect on LPS (0.2 ng/mL) –induced TLR4 activation signal (SEAP) ($P \leq 0.0001$ for all, except for 0.5 µM pixantrone $P \leq 0{,}01$, compared with only LPS-treated cells, presented above each bar). Significant difference within concentrations is shown only in adjacent conditions (bracket). (b) Cytotoxicity, significance compared with LPS-treated cells. (c) Inhibitory effect on PMA (10 ng/mL) -induced activation of TLR4. Significant difference compared with PMA-treated cells, stars above bars; comparison with TAK-242 (500 nM), bracket. (d) Cytotoxicity compared with PMA-treated cells. Significance assessed by using Tukey's test, all data are expressed as mean ± SD, N = 4.

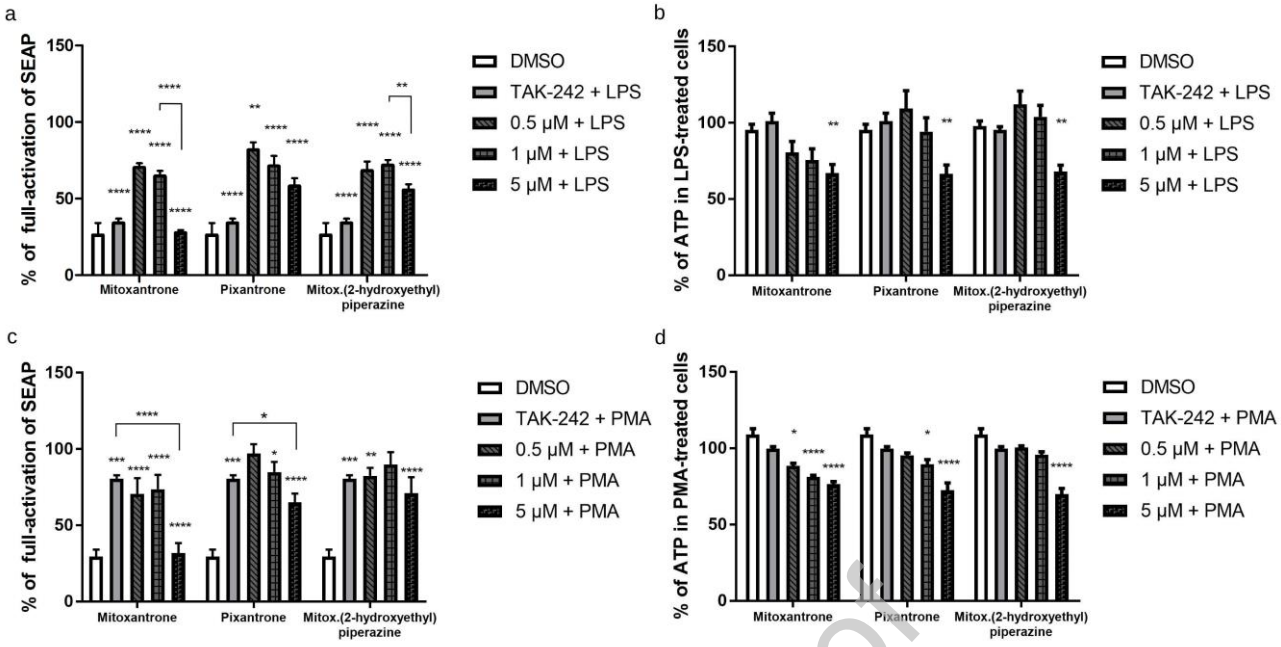

Figure 7. Concentration-response and cytotoxicity of pixantrone and mitoxantrone (2-hydroxyethyl)piperazine on LPS-stimulated mice microglia. Data normalized to the signal of LPS-treated cells (100%; bar not shown). (a) Inhibitory effect on TNFα production. Significant difference, compared to only LPS-treated cells, presented above bars. Significant difference within groups showed only in adjacent bars (bracket). (b) Cytotoxicity, significance comparison to LPS-treated cells. Significance assessed by using Fisher's LSD analysis, data are expressed as mean ± S.E.M., N = 3.

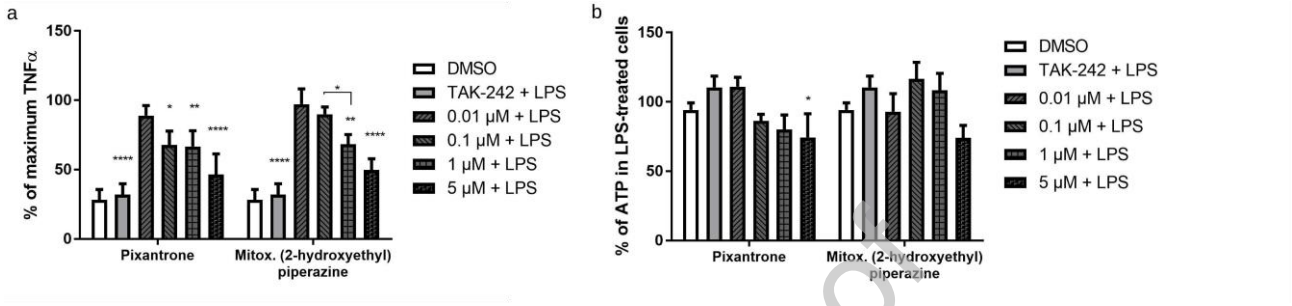

Figure 8. [^{3}H]Mitoxantrone binds specifically to TLR4-expressing membrane fractions, controlled with the known TLR4 antagonist LPS-RS. Specific binding to TLR4 was calculated by subtracting non-specific binding (TLR4-expressing membranes blocked with LPS-RS) from total binding (TLR4-expressing membranes alone). (a) A graph representing all concentrations, (b) represents a zoom of (a) and shows concentration-dependency also at lower concentrations (≤ 125 nM). Data are expressed as mean ± S.E.M., N = 3-4.

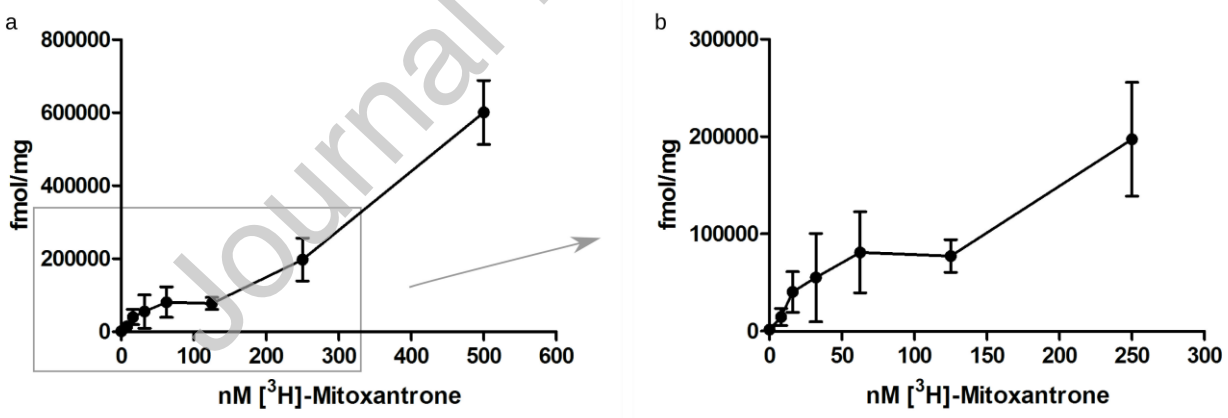

Tables

Table 1. Molecular features of MD-2 loop – TLR4 interactions that were used in the pharmacophore-based virtual screen. HB = hydrogen bond.

Feature type	MD-2	Functional group	TLR4
1. HB donor	Ser-98 -OH	side chain hydroxyl	Arg-289
2. Ionic	Asp-99 -COOH	side chain carboxylate	Arg-289
3. HB acceptor	Asp-99 -C=O- Asp-100	main chain carbonyl	Arg-234
4. HB acceptor / Ionic	Asp-101 -COOH	side chain carboxylate	Ser-317, Arg-264
5. HB acceptor	Asp-101 -C=O- Tyr-102	main chain carbonyl	Arg-264
6. HB donor	Tyr-102 -N- Ser-103	main chain amide nitrogen	Asn-265
7. HB acceptor/donor	Ser-103 -OH	side chain hydroxyl	Asn-265, Glu-266
8. HB acceptor/donor	Arg-106 -$CNNH_4$	side chain guanidinium group	Ser-183, Ser-184

Table 2. Molecular features of LPS – TLR4 interactions (the second TLR4 monomer*) that were used in the pharmacophore-based virtual screen. HB = hydrogen bond.

Feature type	LPS	Atom number in PDB	TLR4
1. HB acceptor	1-PO_4	1011	Lys-341, Lys-362
2. HB acceptor	4´-PO_4	1010	Lys-362, Arg264
3. HB acceptor	C-O-C	1012	Tyr-296
4. HB acceptor	C=O	1006	Arg-264
5. HB donor	R2-OH	1003	Gln-436*

Graphical_abstract